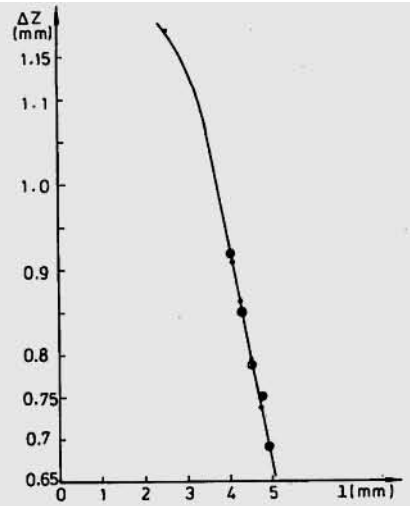

Fig. 2. Softened zone length Δz: experimental data vs empirical model: ⊗, Δz from experimental data; •—•, curve of fitted empirical model for Δz.

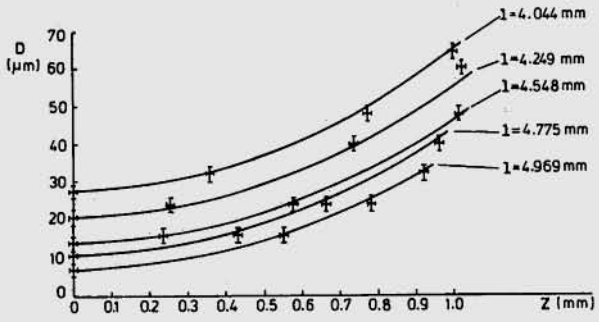

Fig. 3. Taper shape (solid curves), obtained using the empirical Eq. (4) for the softened zone length Δz. Experimental points, with error bars, are superimposed.

Hence the above model is adequate for simulating the evolution of the real taper as the elongation increases. One problem remains, however. As our purpose has been to predict the taper dimensions during the fabrication of the coupler, it would be more convenient to calculate $D(z)$, as given in Eq. (1), as a function of l alone. This implies that γ would be dependent only on l, but Eq. (2) shows that γ is also dependent on Δz. The softened zone length Δz has been found to decrease with increasing l, as can be observed from Table I, since as the molten region is being pulled the reduction in fiber diameter increases the separation between the softened zone and the flame. This in turn leads to a reduced length of the softened zone. Hence an explicit relation between Δz and l is needed. Although in principle the Navier-Stokes equation applies to the formation of the tapered region, the existence of the conical boundaries and of this decreasing softened zone length makes any attempt at such a solution prohibitively difficult. Consequently for the coupler used in this experiment the following equation has been derived, with l and Δz being expressed in millimeters:

$$\Delta z = 0.179 + 1.08[1 + 2(l/5.3)^2] \exp[-2(l/5.3)^2]. \quad (4)$$

Figure 2 is a graph of Eq. (4) with the experimental values of Δz being superimposed for comparison. It is seen that this equation gives a close fit to the experimental data over the coupling region of interest, i.e., for elongation lengths >4 mm.

The corresponding computed curves for the diameter of the fused coupler, plotted against z measured from the waist position, are shown in Fig. 3 together with the experimental points obtained from the microphotographs. The good fit obtained thus justifies quantitatively the use of the above procedure to model the shape of the taper during the coupler fabrication. This modeling procedure consists of assuming a parabolic shape for the taper, and additionally using an empirical equation to model the reduction of the softened zone length during the fabrication.

References

1. J. M. P. Rodrigues, T. S. M. Maclean, B. K. Gazey, and J. F. Miller, "Completely Fused Tapered Couplers: Comparison of Theoretical and Experimental Results," Electron. Lett. **22**, 402 (1986).
2. J. M. P. Rodrigues, "A Study of Fibre Optic Fused Couplers," Ph.D. Thesis, U. Birmingham, U.K. (1985).
3. J. Bures, S. Lacroix, and J. Lapierre, "Analyse d'un coupleur bidirectionnel à fibres optiques monomodes fusionnées," Appl. Opt. **22**, 1918 (1983).

Spectral line profile of turbulent gas

Gao Zhi and J. Qian

Gao Zhi is with Academia Sinica, Institute of Mechanics, Beijing, China. J. Qian is at P.O. Box 142, Branch Box 207, Beijing, China.
Received 18 October 1986.
0003-6935/87/091579-03$02.00/0.

A simple theoretical model is proposed to determine the spectral line profile of a turbulent gas. It is shown that the spectral line profile of a turbulent gas is still a Voigt profile which is a convolution of Lorentzian and Gaussian profiles. Its Lorentzian component is hardly influenced by the turbulent motion. The linewidth of its Gaussian component is $\Delta\nu = \Delta\nu_0[1 + 2\gamma M^2]^{1/2}$. Here $\Delta\nu_0$ is the linewidth of ordinary Doppler broadening due to the thermal motion of molecules, M is the Mach number corresponding to the fluctuation velocity of turbulence, and γ is the ratio of specific heats of the gas. When M is not small, turbulence Doppler broadening is significant.

For the case when the gas has no macroscopic motion, the topic of its spectral line profile has been the content of many textbooks, for example, Refs. 1 and 2. One of the authors has studied the influence of the macroscopic motion of gas on the spectral line profile,[3,4] and it is assumed that the macroscopic motion is laminar. However in practical applications, from the gaseous flows obtained in laboratories to the motion of stellar atmospheres, the turbulent motion is more typical than the laminar motion.[5,6] In this Letter a simple theoretical model is proposed to determine the influence of the turbulent motion on the spectral line profile of a gas. For a turbulent gas the major types of spectral line broadening are still natural line broadening, collision broadening, and Doppler broadening. Ordinary Doppler broadening is due to the microscopic thermal motion of molecules. In the case of a turbulent gas, it is necessary to consider the contribution of macroscopic turbulent motion as well as microscopic thermal motion to Doppler broadening.

In a turbulent gas the total molecular velocity is

$$V = \bar{V} + \tilde{V} + v_t. \quad (1)$$

Here $\bar{V}$ and $\tilde{V}$ are the average velocity and the fluctuation velocity of the turbulent gas, respectively, and v_t is the velocity of microscopic thermal motion. Since Dopper broadening depends on the velocity component along the direction of the light beam, in this Letter all the velocities in Eq. (1) are understood to be the corresponding velocity components along the direction of the light beam, i.e., the projections of the velocity vectors on the direction of the light beam. Of course, the velocity vectors of turbulent motion and thermal motion are not necessarily in the direction of the light beam. Both $\tilde{V}$ and v_t are random variables. Following the argument which led to the Voigt profile,[2,4] it is easy to show that the spectral line profile of a turbulent gas is the following convolution:

$$g(\nu,\nu_0) = \int_{-\infty}^{\infty} g_D(\nu',\nu_0) g_H(\nu,\nu') d\nu'. \tag{2}$$

Here ν_0 is the central frequency of the spectral line profile, ν is the frequency of light, ν' is the Doppler apparent frequency, and

$$g_H(\nu,\nu') = \Delta\nu_H/\{2\pi[(\nu-\nu')^2 + (\Delta\nu_H/2)^2]\} \tag{3}$$

is the Lorentzian profile related to natural line broadening and collision broadening, with $\Delta\nu_H$ being the Lorentzian linewidth. The function $g_D(\nu',\nu_0)$ in Eq. (2) corresponds to Doppler broadening and depends on the distribution function $F(V)$ of the total molecular velocity V in Eq. (1). Generally speaking, $g_D(\nu,\nu_0)$ is not necessarily a Gaussian profile. Only when there is no macroscopic motion, i.e., $\bar{V} = \tilde{V} = 0$, does the distribution function $F(V)$ become the Maxwell distribution of molecular thermal motion, and the $g_D(\nu,\nu_0)$ becomes the well-known Gaussian profile:

$$g_G(\nu,\nu_0) = (1/\Delta\nu_0)(C/\pi)^{1/2} \exp\{-C[(\nu-\nu_0)/\Delta\nu_0]^2\}. \tag{4}$$

Here $C = 4\ln 2 = 2.77259$, and $\Delta\nu_0$ is the ordinary Doppler linewidth due to the microscopic thermal motion of molecules. When there is macroscopic laminar motion, i.e., $\bar{V} \neq 0$ and $\tilde{V} = 0$, the distribution function $F(V)$ and the corresponding function $g(\nu,\nu_0)$ have been discussed in Ref. 4 for several typical laminar flows.

In the case of turbulent flows, for simplicity it is assumed that $\tilde{V} \neq 0$ but $\bar{V} = 0$, i.e., the direction of the light beam is normal to the direction of the average motion of turbulence. Later we discuss the more general case when both $\bar{V}$ and $\tilde{V}$ are not zero. Then the central problem is how to determine the distribution function $\bar{F}(\tilde{V} + v_t)$ of the random velocity $\tilde{V} + v_t$. The distribution function for the velocity v_t of microscopic thermal motion is a Gaussian distribution or a Maxwell distribution. According to the behavior of various two-point correlation functions,[7-9] strictly speaking, the turbulent motion cannot be described as a Gaussian stochastic process. However, most experiments demonstrate that for a fully developed turbulence the distribution function of the fluctuation velocity $\tilde{V}$ itself can be approximately described by a Gaussian distribution.[6-8] There is no correlation between the macroscopic turbulent motion and the microscopic thermal motion; the random variables $\tilde{V}$ and v_t are independent. In the probability theory it is proved that the sum of two independent Gaussian random variables is still a Gaussian random variable.[10] Therefore the distribution function $\bar{F}(\tilde{V} + v_t)$ of the random velocity $\tilde{V} + v_t$ is a Gaussian distribution, and moreover

$$\langle(\tilde{V} + v_t)^2\rangle = \langle\tilde{V}^2\rangle + \langle v_t^2\rangle. \tag{5}$$

Here $\langle \ldots \rangle$ means the statistical average. By using a relevant formula of gas dynamics,[11] from Eq. (5) we have

$$\langle(\tilde{V} + v_t)^2\rangle = \langle v_t^2\rangle(1 + 2\gamma M^2), \qquad M = (\langle\tilde{V}^2\rangle)^{1/2}/a. \tag{6}$$

Here a is the sonic speed of the gas, M is the Mach number corresponding to the fluctuation velocity, and γ is the ratio of the specific heats of the gas. In other words, $\bar{F}(\tilde{V} + v_t)$ is a Maxwell distribution with the equivalent temperature

$$T_e = T(1 + 2\gamma M^2). \tag{7}$$

Here T is the actual temperature of the gas. As a consequence, it is not difficult to prove that the function $g_D(\nu,\nu_0)$ in Eq. (2) now becomes a Gaussian profile and

$$g_D(\nu,\nu_0) = (1/\Delta\nu)(C/\pi)^{1/2} \exp\{-C[(\nu-\nu_0)/\Delta\nu]^2\}. \tag{8}$$

Here $C = 2.77259$ and

$$\Delta\nu = \Delta\nu_0[1 + 2\gamma M^2]^{1/2}, \tag{9}$$

where $\Delta\nu_0$ is the ordinary Doppler linewidth defined in Eq. (4).

When the Mach number M is not small, for example, in the turbulent wake of a supersonic aircraft or in turbulent stellar atmospheres, the influence of turbulence on the spectral line profile cannot be neglected. The typical value of γ is 1.4 (see Ref. 11) according to Eqs. (7) and (9). For $M = 1$ we have $T_e/T = 3.8$ and $\Delta\nu/\Delta\nu_0 = 1.95$; for $M = 0.5$ we have $T_e/T = 1.7$ and $\Delta\nu/\Delta\nu_0 = 1.3$. The spectral line profile is given by Eqs. (2), (3), (8), and (9). When the spectral line profile is applied to the measurement of the temperature of a turbulent gas, the equivalent temperature T_e given by Eq. (7) is obtained instead of the actual temperature T of the gas, so the interpretation of the measurement results should be carefully made. If the actual temperature T can be independently determined by some other methods, the spectral line profile can be applied to the measurement of characteristics of the fluctuation velocity of turbulence.

For the more general case of both $\bar{V}$ amd $\tilde{V}$ being other than zero, the spectral line profile of a turbulent gas can be easily obtained by using the results presented in this Letter together with the method proposed in Ref. 4, substituting $\bar{V}, \tilde{V} + v_t$, and the turbulence Doppler-broadening profile [Eq. (8)] of this Letter for the macroscopic laminar velocity u, the thermal velocity v_T, and the ordinary Gaussian profile [Eq. (2.4)] of Ref. 4, respectively. The key point is that the combined effect of macroscopic fluctuating motion and the molecular thermal motion can be described by the equivalent temperature [Eq. (7)] or the combined Doppler linewidth [Eq. (9)]. The more delicate problem of the influence of temperature or density fluctuation on the spectral line profile of a turbulent gas as well as the non-Gaussian correction are topics for further study.

References

1. D. C. Sinclair and W. F. Bell, *Gas Laser Technology* (Holt, Rinehart, & Winston, New York, 1969).
2. W. Demtroder, *Laser Spectroscopy* (Springer-Verlag, New York, 1981).
3. Zhi Gao, "Gain Saturation in Gas Flow and Chemical Lasers," Sci. Sin. Ser. A **28**, 201 (1985).
4. Zhi Gao, "A Discussion on the Principle of Flow-Velocity and Flow-Pattern Measurements Using Laser Spectral Line Profiles," Acta Mech. Sin. **18**, 215 (1986). (in Chinese)
5. H. Tennekes and J. L. Lumley, *A First Course in Turbulence* (MIT Press, Cambridge, 1972).
6. J. O. Hinze, *Turbulence* (McGraw-Hill, New York, 1975).
7. A. S. Monin and A. M. Yaglom, *Statistical Fluid Mechanics* (MIT Press, Cambridge, 1975).

8. F. Anselmet, Y. Gagne, E. J. Hopfinger, and R. A. Antonia, "High-Order Velocity Structure Functions in Turbulence Shear Flows," J. Fluid Mech. **140,** 63 (1984).
9. R. M. Kerr, "Higher-Order Derivative Correlations and the Alignment of Small-Scale Structures in Isotropic Numerical Turbulence," J. Fluid Mech. **153,** 31 (1985).
10. A. Papoulis, *Probability, Random Variables and Stochastic Process* (McGraw-Hill, New York, 1965).
11. H. W. Liepmann and A. Roshko, *Elements of Gasdynamics* (Wiley, New York, 1957).

High frequency Faraday rotation in FR-5 glass

Michael A. Butler and Eugene L. Venturini

Sandia National Laboratories, Albuquerque, New Mexico 87185.
Received 12 January 1987.
0003-6935/87/091581-02$02.00/0.

Optical materials which exhibit a large Faraday effect can be used as optical isolators, modulators, and high speed switches. The large Faraday effect is commonly obtained by use of magnetic materials[1] or by doping with magnetic ions.[2] In a recent paper[3] it was pointed out that the frequency response of the Faraday effect in such materials depends on the ability of the induced magnetization to follow the rapidly varying applied magnetic field. Thus the Faraday effect is limited by the relaxation of the magnetization of the Faraday material. In this Letter measurement of the Faraday effect in FR-5 glass[2] up to 5 GHz is reported, and factors limiting the response of this material are discussed.

FR-5 glass is a terbium-doped borosilicate glass which has a Verdet constant ~20 times larger than quartz[2] (0.35 min/Oe·cm at 531 nm).[4] The active ion is thought to be Tb^{3+}, and magnetic susceptibility measurements indicate a Tb^{3+} density of 2.5×10^{21} cm^{-3}, assuming all Tb^{3+} ions are in the same magnetic ground state. The temperature dependence of the susceptibility follows a C/T (Curie) curve from 5 to 300 K, suggesting the Tb^{3+} ions are not strongly coupled by dipolar or exchange interactions. The magnetic field dependence of the glass moment at 5 and 7 K follows a Brillouin function from 5 to 50 kOe with a spectroscopic splitting g factor of 2.3 and an angular momentum J of 6. These values were used to calculate the Tb^{3+} concentration quoted above.

Faraday rotation as a function of the frequency of the applied magnetic field was measured using the apparatus[3] shown in Fig. 1. Briefly, the time varying magnetic field is produced at the sample by incorporation of the sample in a microstripline. The sample is a cube, 3.5 mm on each side, whose dimensions match the width of the microstripline. Calculations show that the magnetic field, typically 0.1 G rms, is uniform along the light beam in the sample. The 531-nm line of a krypton laser is passed through the sample collinear with the applied field, and the polarization modulation is converted to amplitude modulation by the analyzer. The signal is detected by a fast photodiode and spectrum analyzer.

The frequency dependence of the Faraday effect in FR-5 glass is shown in Fig. 2. The observed effect corresponds to a modulation of the polarization direction of three microradians. It has been shown[3] that Faraday rotation in a paramagnetic material will have a frequency dependence given by

$$\theta(\omega) = \theta(o)/\sqrt{1 + \omega^2\tau^2}, \quad (1)$$

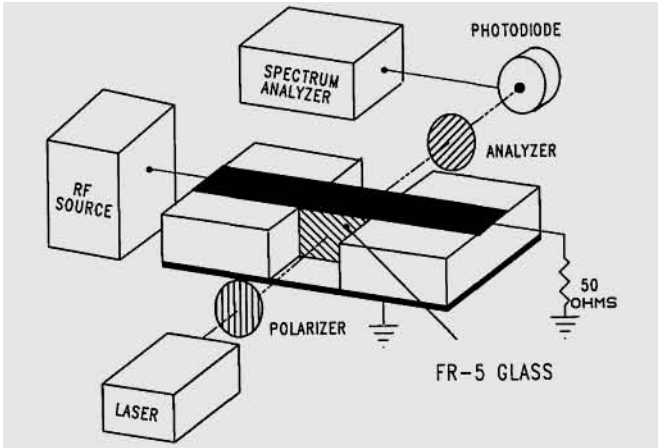

Fig. 1. Experimental apparatus for measuring the frequency dependence of the optical Faraday effect.

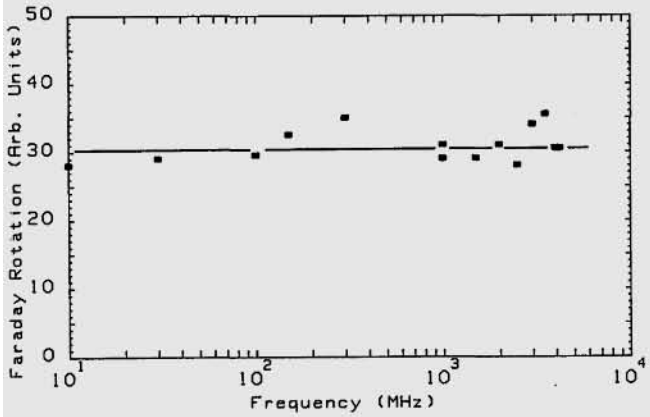

Fig. 2. Frequency dependence of the Faraday effect in FR-5 glass. The magnitude of the effect corresponds to modulation of the polarization direction by three microradians.

where τ is a relaxation time which describes the response of the magnetization to the applied magnetic field. Since the observed Faraday rotation is independent of frequency up to at least 5 GHz, this relaxation time must be $<3 \times 10^{-11}$ s.

Two mechanisms can contribute to the relaxation process: transfer of energy between terbium magnetic moments via the dipolar interaction and transfer of energy from the terbium moments to the lattice via spin–lattice interactions. The size of the dipolar interactions can be estimated from the magnetic susceptibility measurements, and they do not appear to be large enough to explain the observed relaxation time. The most likely explanation is a rapid spin–lattice relaxation process.

The Tb^{3+} ion has a $J = 6$ ground state with a large orbital component. EPR measurements of the relaxation time for Tb^{3+} ions in $CaWO_4$ (Ref. 5) show an exponential dependence on temperature given by

$$T_1(s) = 3.3 \times 10^{-13} \exp(14.3/T), \quad (2)$$

where the data were taken between 5 and 30 K. Extrapolation of these data to room temperature suggests a spin–lattice relaxation time of the order of 3.5×10^{-13} s or a roll-off frequency for the Faraday effect measurements of several hundred gigahertz. We expect a similar rapid spin–lattice relaxation in FR-5 glass. Such a very rapid relaxation time is